

Energetic Hydrazine-Based Salts with Nitrogen-Rich and Oxidizing Anions

Carles Miró Sabaté,^{*[a]} Henri Delalu,^[a] and Erwann Jeanneau^[b]

Abstract: 1,1,1-Trimethylhydrazinium iodide ($[(\text{CH}_3)_3\text{N}-\text{NH}_2]\text{I}$, **1**) was reacted with a silver salt to form the corresponding nitrate ($[(\text{CH}_3)_3\text{N}-\text{NH}_2][\text{NO}_3]$, **2**), perchlorate ($[(\text{CH}_3)_3\text{N}-\text{NH}_2][\text{ClO}_4]$, **3**), azide ($[(\text{CH}_3)_3\text{N}-\text{NH}_2][\text{N}_3]$, **4**), 5-amino-1*H*-tetrazolate ($[(\text{CH}_3)_3\text{N}-\text{NH}_2][\text{H}_2\text{N}-\text{CN}_4]$, **5**), and sulfate ($[(\text{CH}_3)_3\text{N}-\text{NH}_2][\text{SO}_4]\cdot 2\text{H}_2\text{O}$, **6**·2H₂O) salts. The metathesis reaction of compound **6**·2H₂O with barium salts led to the formation of the corresponding picrate ($[(\text{CH}_3)_3\text{N}-\text{NH}_2][(\text{NO}_2)_3\text{Ph}-\text{O}]$, **7**), dinitramide ($[(\text{CH}_3)_3\text{N}-\text{NH}_2][\text{N}(\text{NO}_2)_2]$, **8**), 5-nitrotetrazolate ($[(\text{CH}_3)_3\text{N}-\text{NH}_2][\text{O}_2\text{N}-\text{CN}_4]$, **9**), and nitroformate ($[(\text{CH}_3)_3\text{N}-\text{NH}_2][\text{C}(\text{NO}_2)_3]$, **10**) salts. Compounds **1–10**

were characterized by elemental analysis, mass spectrometry, infrared/Raman spectroscopy, and multinuclear NMR spectroscopy (¹H, ¹³C, and ¹⁵N). Additionally, compounds **1**, **6**, and **7** were also characterized by low-temperature X-ray diffraction techniques (XRD). Ba(NH₄)(NT)₃ (NT = 5-nitrotetrazole anion) was accidentally obtained during the synthesis of the 5-nitrotetrazole salt **9** and was also characterized by low-temperature XRD. Further-

more, the structure of the $[(\text{CH}_3)_3\text{N}-\text{NH}_2]^+$ cation was optimized using the B3LYP method and used to calculate its vibrational frequencies, NBO charges, and electronic energy. Differential scanning calorimetry (DSC) was used to assess the thermal stabilities of salts **2–5** and **7–10**, and the sensitivities of the materials towards classical stimuli were estimated by submitting the compounds to standard (BAM) tests. Lastly, we computed the performance parameters (detonation pressures/velocities and specific impulses) and the decomposition gases of compounds **2–5** and **7–10** and those of their oxygen-balanced mixtures with an oxidizer.

Keywords: crystal structures · density functional calculations · energetic compounds · hydrazines · NMR (multinuclear) spectroscopy

Introduction

Liquid hydrazines (e.g., hydrazine, monomethylhydrazine, and 1,1-dimethylhydrazine) are widely used in rocket fuels in combination with strong oxidizers (e.g., nitrogen tetroxide (NTO), white fuming nitric acid (WFNA), or red fuming nitric acid (RFNA)) (Figure 1).^[1–4] Unfortunately, hydrazine



Figure 1. Commonly used oxidizers: nitrogen tetroxide (NTO), white/red fuming nitric acid (WFNA/RFNA), ammonium nitrate (AN), and ammonium dinitramide (ADN).

and its liquid covalent derivatives are highly toxic and volatile, and they can form explosive mixtures with air.^[5] In this context, salt-based energetic materials are at the center of attention in view of their potential to replace liquid hydrazines^[6–9] due to their lower vapor pressure (which essentially eliminates the risk of exposure through inhalation), their higher density (which is directly proportional to the energetic performance of the materials), and their high thermal and chemical stabilities.^[6–13]

Recently, we reported on a series of energetic salts based on the 1,2-dimethylhydrazine cation, which have low sensitivities to classical stimuli, are less toxic than liquid hydrazines, perform better than 1,3,5-trinitrotoluene (TNT), and have good thermal and chemical stabilities.^[14] Also recently, a series of energetic salts based on the $[(\text{CH}_3)_2\text{N}(\text{R})\text{NH}_2]^+$ cation (R = amino and alkyl groups) were reported.^[8,9,15] The high thermal robustness and interesting energetic properties of this type of materials attracted our attention to the $[(\text{CH}_3)_3\text{N}-\text{NH}_2]^+$ cation. The synthesis of this cation was reported as early as 1957 by Sisler and Omietanski^[16] by alkylation of the corresponding hydrazine. The first report on an energetic salt of the $[(\text{CH}_3)_3\text{N}-\text{NH}_2]^+$ cation was that of the nitrate salt, which appeared as late as 1992. This compound was synthesized by amination of trimethylamine using hydroxylamine-*O*-sulfonic acid and was only characterized by NMR and infrared spectroscopies.^[17] Reports on the azide and azobistetrazolate salts followed in 1999 and 2001, respectively.^[18] Although both compounds were properly char-

[a] Dr. C. M. Sabaté, Dr. H. Delalu
Laboratoire Hydrazines et Composés Énergétiques Polyazotés
UMR 5278/CNRS/UCBL/CNES/SME-SAFRAN
Université Claude Bernard Lyon 1
3è étage, 22, av. Gaston Berger, 69622 Villeurbanne (France)
Fax: (+33)472-431-291
E-mail: carlos.miro-sabate@univ-lyon1.fr

[b] Dr. E. Jeanneau
Centre de Diffractométrie Henri Longchambon
Université Claude Bernard Lyon 1
43 Bd. du 11 novembre 1918, 69622 Villeurbanne (France)
Fax: (+33)472-431-160

Supporting information for this article is available on the WWW under <http://dx.doi.org/10.1002/asia.201200437>.

acterized, detailed information about their thermal stabilities, their sensitivities towards classical stimuli, and their energetic performances appears to be missing in the literature. Lastly, the dicyanamide and nitrocyanamide salts were recently investigated by Shreeve et al.^[9] The latter compounds were characterized by analytical and spectroscopic methods, and their energetic properties suggest that these materials might have potential as hypergolic ionic liquids. In this context, we would like to present our results on the synthesis, characterization, and energetic properties of energetic salts of the $[(\text{CH}_3)_3\text{N}-\text{NH}_2]^+$ cation with nitrogen-rich and oxidizing anions.

Results and Discussion

Synthesis

1,1-Dimethylhydrazine was reacted with methyl iodide in THF according to a recently published procedure^[9] to form the corresponding iodide salt $[(\text{CH}_3)_3\text{N}-\text{NH}_2]\text{I}$, **1**, Scheme 1). Compound **1** was then reacted with silver salts in water or alcohol, leading to the formation of the nitrate $[(\text{CH}_3)_3\text{N}-\text{NH}_2][\text{NO}_3]$, **2**, perchlorate $[(\text{CH}_3)_3\text{N}-\text{NH}_2][\text{ClO}_4]$, **3**, azide $[(\text{CH}_3)_3\text{N}-\text{NH}_2][\text{N}_3]$, **4**, 5-amino-1*H*-tetrazolate $[(\text{CH}_3)_3\text{N}-\text{NH}_2][\text{H}_2\text{N}-\text{CN}_4]$, **5**, and sulfate $[(\text{CH}_3)_3\text{N}-\text{NH}_2][\text{SO}_4]\cdot 2\text{H}_2\text{O}$, **6** $\cdot 2\text{H}_2\text{O}$ salts. Subsequently, compound **6** $\cdot 2\text{H}_2\text{O}$ was reacted in water or alcohol with barium salts to form the corresponding picrate $[(\text{CH}_3)_3\text{N}-\text{NH}_2][(\text{NO}_2)_3\text{Ph}-\text{O}]$, **7**, dinitramide $[(\text{CH}_3)_3\text{N}-\text{NH}_2][\text{N}(\text{NO}_2)_2]$, **8**, 5-nitrotetrazolate $[(\text{CH}_3)_3\text{N}-\text{NH}_2][\text{O}_2\text{N}-\text{CN}_4]$, **9**, and nitroformiate $[(\text{CH}_3)_3\text{N}-\text{NH}_2][\text{C}(\text{NO}_2)_3]$, **10** salts. Except for salts **7** and **10**, which are bright yellow compounds, the remainder of the materials are colorless. Furthermore, salts **1**–**10** are stable to hydrolysis and are readily soluble in water, DMSO, ethanol, and acetone, less soluble in solvents such as isopropanol and THF, and insoluble in dichloromethane and ether. Lastly, during the synthesis of salt **9** single crystals of the ammonium/barium double salt of

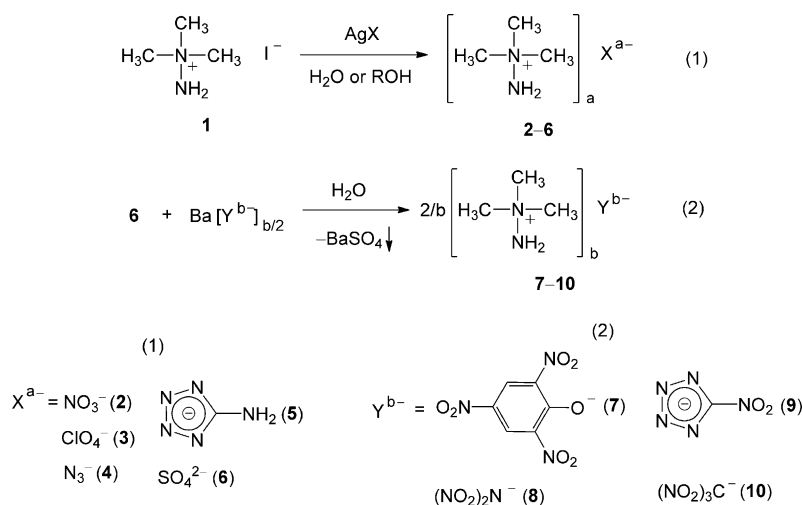
the 5-nitrotetrazole anion (i.e., $\text{Ba}(\text{NH}_4)(\text{NT})_3$, NT = 5-nitrotetrazole anion) were obtained (see X-ray discussion below).

Spectroscopic Analysis

The most intense bands in the Raman spectra of salts **2**–**10** correspond to the vibration modes of the anions and are observed at 1052 cm^{-1} (nitrate, $\nu(\text{NO}_3)$),^[19] 935 and 462 cm^{-1} (perchlorate, $\nu(\text{ClO}_4)$ and $\delta(\text{ClO}_4)$),^[20] 1328 cm^{-1} (azide, $\nu(\text{N}_3)$),^[21] 749 and 1046 cm^{-1} (5-amino-1*H*-tetrazolate, $\tau(\text{NH}_2)$ and $\nu(\text{N}_{\text{ring}}-\text{N}_{\text{ring}})$),^[22] 978 cm^{-1} (sulfate, $\nu(\text{SO}_4)$),^[23] 1309 , 1329 , 1347 , and 1365 cm^{-1} (picrate, $\nu(\text{NO}_2)$),^[24] 827 and 1328 cm^{-1} (dinitramide, $\delta(\text{NO}_2)$ and $\nu(\text{NO}_2)$),^[21] 1024 , 1060 , and 1423 (5-nitrotetrazolate, $\delta(\text{NO}_2)$ and $\nu(\text{NO}_2)$),^[25] and 868 and $1271/1378\text{ cm}^{-1}$ (nitroformiate, $\delta(\text{NO}_2)$ and $\nu(\text{NO}_2)$).^[26] Table S1 in the Supporting Information contains a summary of the (scaled) calculated frequencies with infrared intensities and Raman scattering activities along with the experimental averaged values of the salts of the $[(\text{CH}_3)_3\text{N}-\text{NH}_2]^+$ cation studied in this work. The most intense bands for the vibrational modes of the $[(\text{CH}_3)_3\text{N}-\text{NH}_2]^+$ cation in the Raman spectra are the C–N and N–N stretching modes, found experimentally in the range 750 to 945 cm^{-1} .

On the other hand, the bands of the anion in the infrared spectra of salts **2**–**10** are obscured by the vibrational modes of the $[(\text{CH}_3)_3\text{N}-\text{NH}_2]^+$ cation. These spectra are dominated by strong C–N stretching bands at approximately 950 cm^{-1} and signals of medium intensity at 1060 and 1150 cm^{-1} (torsion modes of the $-\text{NH}_2$ and $-\text{CH}_3$ groups). The rest of the bands have lower intensities and can be assigned as follows: 3270 – 3345 cm^{-1} ($-\text{NH}_2$ group symmetric and asymmetric stretches), 2965 – 3145 cm^{-1} ($-\text{CH}_3$ group symmetric and asymmetric stretches), 1475 – 1615 cm^{-1} (in-plane bending modes of the $-\text{NH}_2$ and $-\text{CH}_3$ groups), 1315 – 1425 cm^{-1} (out-of-plane bending modes of the $-\text{NH}_2$ and $-\text{CH}_3$ groups), 1060 – 1275 cm^{-1} (torsion modes of the $-\text{NH}_2$ and $-\text{CH}_3$ groups), and $< 500\text{ cm}^{-1}$ (C–N–N and C–N–C in-plane bending modes).^[27]

The structure of the $[(\text{CH}_3)_3\text{N}-\text{NH}_2]^+$ cation was also characterized in solution using multinuclear NMR spectroscopy (^1H , ^{13}C , and ^{15}N). Table 1 shows a summary of the NMR measurements. The ^1H NMR spectra of salts **1**–**10** (in $[\text{D}_6]\text{DMSO}$) show two resonances: that of the $-\text{CH}_3$ groups at approximately 3.25 ppm and that of the $-\text{NH}_2$ groups, which appear as broad signals in the range between about 6.00 and 6.20 ppm . In the ^{13}C NMR spectra, the $-\text{CH}_3$



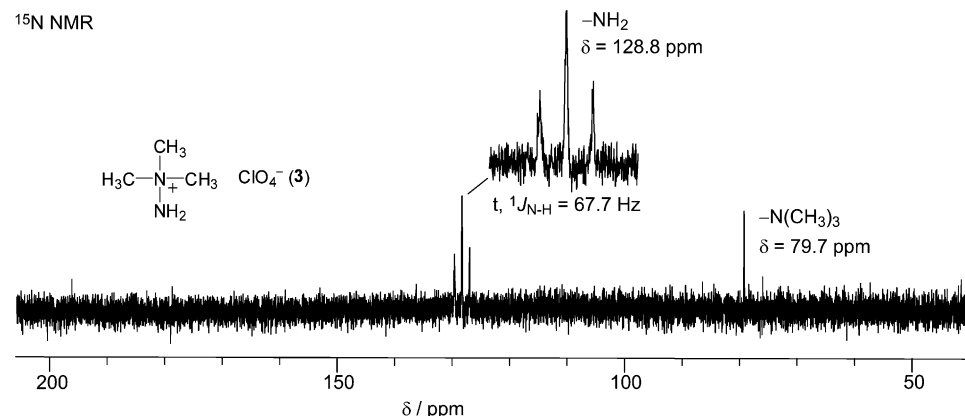
Scheme 1. Synthesis of salts of the $[(\text{CH}_3)_3\text{N}-\text{NH}_2]^+$ cation.

Table 1. ^1H , ^{13}C , and ^{15}N NMR chemical shifts (ppm) of the $[(\text{CH}_3)_3\text{N}-\text{NH}_2]^+$ cation in compounds **1–10**.^[a]

	^1H NMR		^{13}C NMR	^{15}N NMR ^[b]	
	$-\text{CH}_3$	$-\text{NH}_2$	$-\text{CH}_3$	$-\text{N}(\text{CH}_3)_3$	$-\text{NH}_2$
1	3.28	6.10	57.2		
2	3.26	6.11	57.2		
3	3.24	6.04	57.3	+79.7	+128.8 ($^1J_{\text{N-H}}=67.7$ Hz)
4	3.22	6.22	57.2		
5	3.26	6.11	57.2		
6	3.25	6.09	57.2		
7	3.25	6.09	57.2		
8	3.25	6.07	57.3		
9	3.26	6.10	57.3		
10	3.25	6.09	57.2		

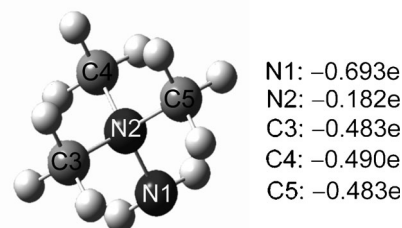
[a] in $[\text{D}_6]\text{DMSO}$; [b] ammonia was used as an external standard.

groups of compounds **1–10** show very consistent resonances at about 57.2 ppm. Additionally, we measured the ^{15}N NMR spectrum of the perchlorate salt (**3**) as a representative example of a salt containing the $[(\text{CH}_3)_3\text{N}-\text{NH}_2]^+$ cation (Figure 2). The nitrogen atom of the $-\text{N}(\text{CH}_3)_3$ moiety resonates at +79.7 ppm (ammonia as external standard), and no multiplicity was observed, whereas the $-\text{NH}_2$ group resonates at +128.8 ppm with a coupling constant $^1J_{\text{N-H}}$ of 67.7 Hz.

Figure 2. ^{15}N NMR spectrum of compound **3** in $[\text{D}_6]\text{DMSO}$ (ammonia as an external reference).

NBO Analysis and Crystal Structures

The optimized structure of the $[(\text{CH}_3)_3\text{N}-\text{NH}_2]^+$ cation (obtained from density functional theory calculations at the B3LYP/6-31+G(d,p) level) was used for natural bond orbital (NBO) calculations (Figure 3).^[28] The amino group nitrogen atom (N1) has the largest negative charge ($-0.693e$) and is involved in strong hydrogen bonding to anions and cations (see the discussion below). On the other hand, the ammonium nitrogen atom bears the lowest negative charge (ca. $-0.182e$). Lastly, the three methyl group carbon atoms have comparable negative charges of about $-0.485e$.

Figure 3. Optimized geometry and natural bond orbital (NBO) charge distribution of the $[(\text{CH}_3)_3\text{N}-\text{NH}_2]^+$ cation (B3LYP/6-31+G(d,p)).

The disorder found in the crystal structure of salt **1** accounts for the significant differences in the bond lengths of this compound with the analogous distances in salts **6** and **7**. With the exception of compound **1**, the bond lengths in the cation in the crystal structures of the salts of the $[(\text{CH}_3)_3\text{N}-\text{NH}_2]^+$ cation are in the expected range for N–N and C–N single bonds, while the bond angles are close to the expected 109.5° for a tetrahedral geometry (Table 2). The computed values (B3LYP and MP2) for the gas-phase structure of the $[(\text{CH}_3)_3\text{N}-\text{NH}_2]^+$ cation are in good agreement with those of the solid state. Compound **1** crystallizes in a tetragonal cell (Figure 4). The substituents around the $[(\text{CH}_3)_3\text{N}-\text{NH}_2]^+$ cation are disordered so that the probability of each substituent being a $-\text{CH}_3$ group is 75%, whereas that of it being a $-\text{NH}_2$ group is 25%. The structure does not contain any significant hydrogen bonds; however, long contacts between the hydrogen atoms of the $-\text{NH}_2$ groups and the iodine anions exist ($\text{N}\cdots\text{I} = 3.677(15)$ Å). These contacts describe ring graph sets^[29] with the label R1,2(12) and are shown in Figure 4.

Table 2. Selected bond lengths (Å) and angles ($^\circ$) (from the X-ray crystal structures) for salts of the $[(\text{CH}_3)_3\text{N}-\text{NH}_2]^+$ cation and comparison with the computed values (from chemical quantum calculations).^[a]

Parameter	1	6 (A)	6 (B)	7	B3LYP	MP2
N1–N2	1.556(7)	1.446(8)	1.447(7)	1.448(2)	1.452	1.451
N2–C3	1.463(6)	1.521(11)	1.504(8)	1.501(3)	1.508	1.501
N2–C4	1.463(6)	1.491(10)	1.495(10)	1.498(3)	1.507	1.501
N2–C5	1.463(6)	1.475(9)	1.467(10)	1.487(3)	1.510	1.502
N1–N2–C3	105.7(1)	106.9(6)	107.7(6)	107.2(2)	106.5	106.7
N1–N2–C4	111.2(1)	107.9(6)	108.1(6)	109.0(2)	106.5	106.7
C3–N2–C4	108.2(1)	109.4(7)	110.1(6)	110.0(2)	113.3	113.1
N1–N2–C5	111.2(1)	113.1(6)	110.9(5)	110.4(2)	109.8	109.6
C3–N2–C5	108.2(1)	110.5(7)	110.2(6)	110.3(2)	110.3	110.3
C4–N2–C5	111.9(1)	108.8(6)	109.8(6)	109.6(2)	110.3	110.3

[a] See Figure 3 for the labeling scheme.

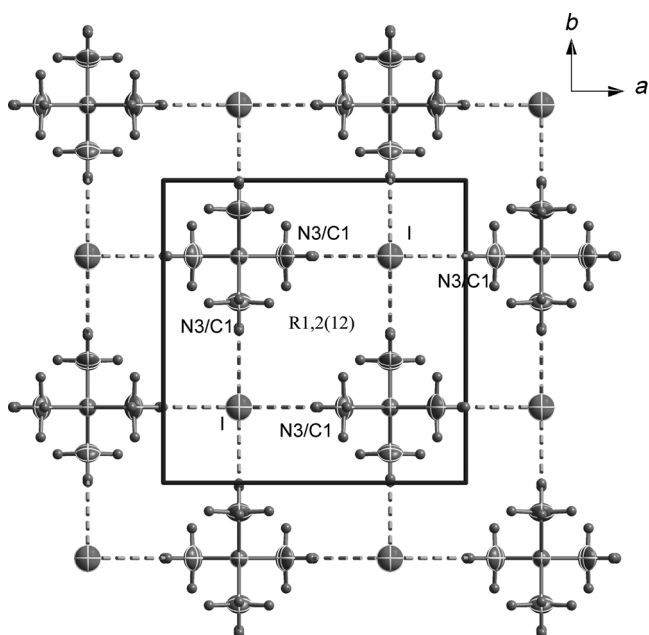


Figure 4. View along the *c*-axis of the unit cell of compound **1** with the iodine–hydrogen contacts (dotted lines). The substituents around the $[(\text{CH}_3)_3\text{N}-\text{NH}_2]^+$ cation are disordered (occupancy: 75/25% ($-\text{CH}_3/-\text{NH}_2$)).

The sulfate salt of the $[(\text{CH}_3)_3\text{N}-\text{NH}_2]^+$ cation formed as a dihydrate ($6 \cdot 2\text{H}_2\text{O}$). In the solid state, the compound is involved in four unclassical C–O and seven classical N–O and O–O hydrogen bonds (Table S3 in the Supporting Information), which form D1,1(2) dimeric graph-sets (primary level). As shown in Figure 5, the oxygen atoms of the sulfate anions are involved in hydrogen bonding to the cations and to the molecules of water of crystallization. At the secondary level, these hydrogen bonds describe dimeric patterns of the type D1,2(3) and D2,2(5), chain motifs with the descriptors C1,2(6) and C2,2(X) ($X=6, 8$), and R1,2(6), R2,1(4),

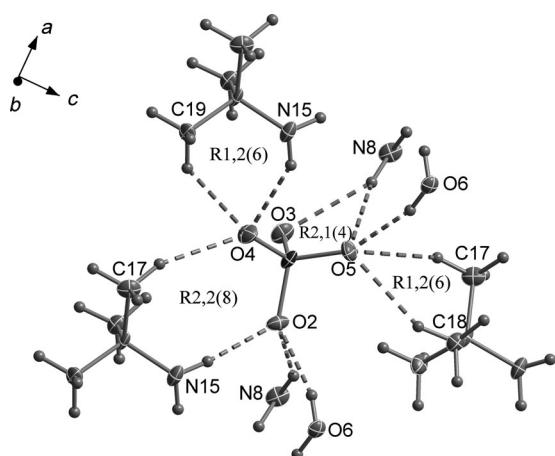


Figure 5. Packing around the anion with the hydrogen bonding (dotted lines) and the ring graph sets in the crystal structure of compound $6 \cdot 2\text{H}_2\text{O}$. For two of the cations, only the amino groups ($\text{N}8\text{H}_2$) are shown for simplicity.

and R2,2(8) ring graph sets. The three types of ring graph sets found in the structure of $6 \cdot 2\text{H}_2\text{O}$ are shown in Figure 5. For example, the R2,2(8) ring patterns are formed by two hydrogen bonds between one cation and two oxygen atoms of the same anion ($\text{C}17 \cdots \text{O}4 = 3.242(9)$ and $\text{N}15 \cdots \text{O}2 = 3.053(9)$ Å), and the R1,2(6) patterns involve the combination of two hydrogen bonds between one cation and the same oxygen atom of the anion ($\text{C}17 \cdots \text{O}5^i = 3.315(9)$ and $\text{C}18 \cdots \text{O}5^i = 3.272(9)$ Å; symmetry code: (i) $-0.5 + x, 1.5 - y, -0.5 + z$).

Figure 6 shows a view of the unit cell of compound $6 \cdot 2\text{H}_2\text{O}$ along the *a*-axis with the hydrogen bonding (dotted lines). One of the two molecules of water of crystallization is involved in hydrogen bonding, whereas the other one does not participate in any significant interaction and simply occupies the voids between cations. The C1,2(6) and C2,2(X) ($X=6, 8$) infinite chains mentioned above extend along the *c*-axis and keep the structure together.

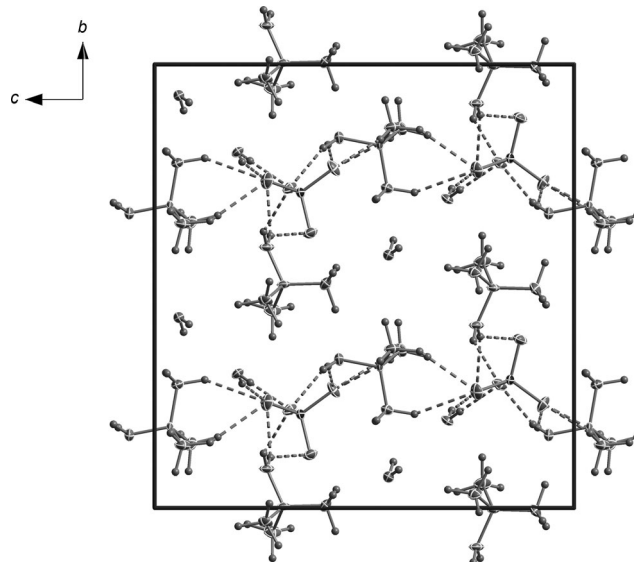


Figure 6. View along the *a*-axis of the unit cell of compound $6 \cdot 2\text{H}_2\text{O}$ with the hydrogen bonding (dotted lines).

Compound **7** crystallizes as the anhydrous material with one cation and one anion in the asymmetric unit. The compound is involved in the formation of one classical N \cdots O and five unclassical C \cdots O hydrogen bonds. At the primary level, only D1,1(2) dimeric interactions are formed, which combine at the secondary level to form chain patterns of the type C2,2(X) ($X=10, 12$) and ring graph sets with the labels R1,2(6), R2,2(X) ($X=8, 10$), R2,4(X) ($X=8, 12$), and R4,4(X) ($X=16, 20, 24$). Figure 7 shows some of the ring hydrogen-bonding networks found in the structure of the compound. For example, the methyl groups of two cations interact with the oxygen atoms of two anions ($\text{C}4 \cdots \text{O}21^i = 2.490(2)$ and $\text{C}4 \cdots \text{O}21^{iii} = 2.531(2)$ Å; symmetry codes: (i) $-x, 2-y, 2-z$; (iii) $x, y, -1+z$), forming R2,4(8) graph sets, and one of the unclassical hydrogen bonds combines

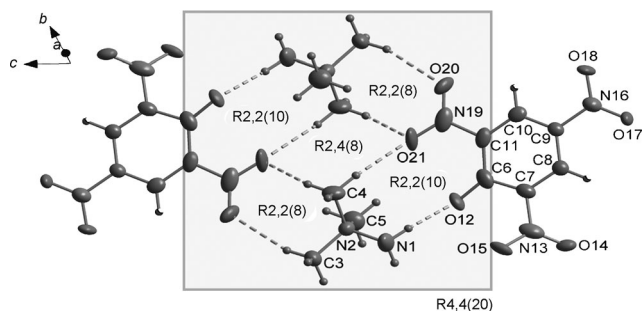


Figure 7. Labeling scheme and ring graph sets (the hydrogen bonds are represented by dotted lines) in the crystal structure of compound **7**.

with the classical hydrogen bond ($C3 \cdots O20^i = 3.517(3)$ and $N1 \cdots O12^{iii} = 2.838(3)$ Å) to form the R4,4(20) networks.

Figure 8 shows a view of the unit cell of compound **7**. The picrate anions form wavy layers, which are linked to each other by hydrogen bonding to the cations. In a layer, two methyl groups of the cation form hydrogen bonds with the same oxygen atom of one of the nitro groups ($C4 \cdots O21^i = 3.391(3)$ and $C5 \cdots O21^i = 3.484(3)$ Å), leading to the formation of R1,2(6) motifs.

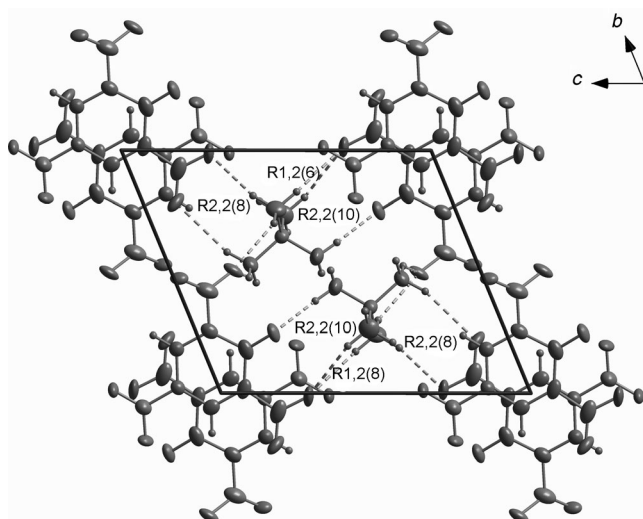


Figure 8. Unit cell of compound **7** (view along the *a*-axis) with the ring graph sets (the hydrogen bonds are represented by dotted lines).

As mentioned above, single crystals of $Ba(NH_4)(NT)_3$ ($NT = 5$ -nitrotetrazole anion) were obtained during the synthesis of compound **9**. $Ba(NH_4)(NT)_3$ is a mixed salt composed of three 5-nitrotetrazole anions, one barium cation, and one ammonium cation so that the overall charge is zero. Unfortunately, the quality of the crystals did not allow us to localize the hydrogen atoms of the ammonium cation. The compound crystallizes in a cubic cell, and the 5-nitrotetrazole anions are disordered so that two possible orientations are possible with the same probability. Figure 9 shows the disorder of the anion in the structure of the compound. A symmetry plane along the C–N bond makes both halves of

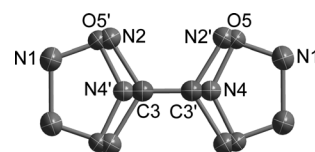


Figure 9. Disorder in the anion in the crystal structure of $Ba(NH_4)(NT)_3$.

the anion identical, and the disorder in the anion is characterized by two possible orientations twisted by 180° .

The unit cell of $Ba(NH_4)(NT)_3$ (Figure 10) is made up of $8 \times 1/8 =$ one Ba^{2+} cation (occupying the vertices), $12 \times 1/4 =$ three disordered 5-nitrotetrazole anions (occupying the mid-points of the sides), and one ammonium cation (occupying the center).

As illustrated in Figure 11, the barium cations coordinate to the 5-nitrotetrazole anions, which act as bidentate ligands. The coordination number around the cations is twelve and completed by interactions to six symmetrically equivalent anions with $Ba \cdots N5 = 2.916(7)$ and $Ba \cdots O3 = 3.056(7)$ Å.

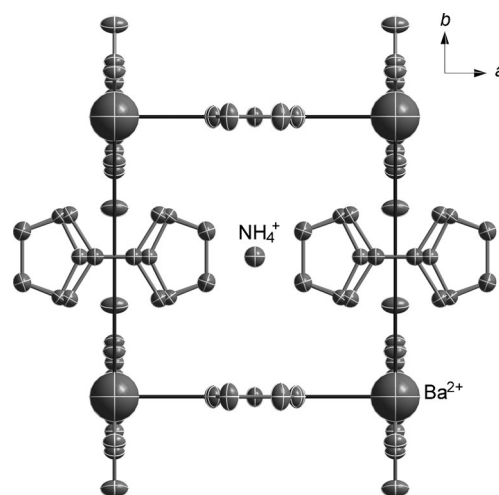


Figure 10. View along the *c*-axis of the unit cell of $Ba(NH_4)(NT)_3$ with the disordered 5-nitrotetrazole anions (ellipsoid model) and the barium cations (ball-and-stick model). The hydrogen atoms around the ammonium cation could not be found.

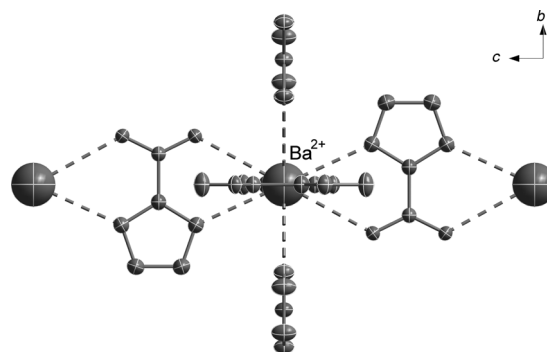


Figure 11. Coordination around the Ba^{2+} cations (dotted lines) in the crystal structure of $Ba(NH_4)(NT)_3$ (view along the *a*-axis). Only one of the two possible orientations of the 5-nitrotetrazole anions is shown.

This results in the formation of infinite (coordination) chains along all three axes, with the ammonium cations occupying the voids between anions.

Physical, Chemical, and Energetic Properties

The sensitivities of compounds **2–5** and **7–10** towards fast heating without confinement where evaluated by burning the materials with a Bunsen burner (“flame test”). Additionally, we assessed the thermal stabilities of all compounds by means of differential scanning calorimetry (DSC) measurements. We then calculated the standard enthalpies (H) and standard free energies (G) of all compounds in this work using the modified complete basis set (CBS-4M) method (Supporting Information, Table S4). These values were then used to estimate the formation energies and enthalpies of compounds **2–5** and **7–10**. Subsequently, we used the calculated formation energies and the EXPLO5 software^[30] to estimate the detonation parameters of salts **2–5** and **7–10**. Additionally, we simulated formulations of compounds **2–5** and **7–10** with oxidizers, namely ammonium nitrate (AN) and ammonium dinitramide (ADN), and also predicted the detonation parameters of the mixtures. The results of these measurements and calculations are summarized in Tables 3 and 4 and in the Supporting Information (Tables S5 and S6).

The “flame tests” resulted in slow burning for the less energetic picrate salt **7**, normal burning for the more energetic compounds **2**, **4**, and **5** and fast burning/deflagration for the better oxygen-balanced salts **3**, **8**, **9**, and **10**. On the other hand, the DSC measurements showed a defined melting for compounds **4** and **7** at 182 and 238 °C, respectively, whereas the remainder of the salts melted with concomitant decomposition. Salts **8** and **10** have low thermal stabilities and decompose sharply at 155 and 137 °C, respectively. The rest of the salts have good to excellent thermal stabilities with the

Table 3. Physical, chemical and thermodynamic properties of salts of the $[(\text{CH}_3)_3\text{N}-\text{NH}_2]^+$ cation.

	2	3	4	5	7	8	9	10
Formula	$\text{C}_3\text{H}_{11}\text{N}_3\text{O}_3$	$\text{C}_3\text{H}_{11}\text{N}_2\text{ClO}_4$	$\text{C}_3\text{H}_{11}\text{N}_3$	$\text{C}_4\text{H}_{13}\text{N}_7$	$\text{C}_6\text{H}_{13}\text{N}_3\text{O}_7$	$\text{C}_3\text{H}_{11}\text{N}_3\text{O}_4$	$\text{C}_4\text{H}_{11}\text{N}_7\text{O}_2$	$\text{C}_4\text{H}_{11}\text{N}_3\text{O}_6$
Mol. Mass [g mol ⁻¹]	137.14	174.58	117.15	159.19	303.23	181.15	189.18	225.16
T_m [°C] ^[a]	–	–	182	–	238	–	–	–
T_d [°C] ^[b]	258	322	216	250	264	155	175	137
$N+O$ [%] ^[c]	66	53	60	62	60	74	69	74
Ω [%] ^[d]	–99	–64	–157	–145	–92	–66	–97	–53
ρ [g cm ⁻³] ^[e]	1.437	1.589	1.217*	1.439	1.573	1.497	1.479	1.603
$\Delta_f H^\circ$ (g, Cat ⁺)/kJ mol ⁻¹ ^[f]	759	759	759	759	759	759	759	759
$\Delta_f H^\circ$ (g, An ⁻)/kJ mol ⁻¹ ^[f]	–312	–276	192	175	–370	–122	104	–217
ΔU_L /kJ mol ⁻¹ ^[g]	537	517	536	516	447	505	497	485
ΔH_L /kJ mol ⁻¹ ^[g]	542	522	539	521	452	510	502	490
$\Delta_f H^\circ$ (s)/kJ mol ⁻¹ ^[h]	–96	–39	169	247	–243	–73	212	–96
$\Delta_f U^\circ$ (s)/kJ kg ⁻¹ ^[h]	–547	–101	1615	1706	–698	–266	1254	–464

[a] Melting point (DSC onset, measurement at $\beta=5^\circ\text{C min}^{-1}$); [b] decomposition point (DSC onset, measurement at $\beta=5^\circ\text{C min}^{-1}$); [c] combined nitrogen and oxygen contents; [d] oxygen balance; [e] density (from the crystal structure or from the picnomet measurements), *density of compound **4** from ref. [18a]; [f] standard (gas phase) heats of formation of the cation (Cat⁺) and of the anion (An⁻); [g] (solid-phase) lattice energies and lattice enthalpies; [h] standard (solid-phase) formation heats/energies of the ionic species.

Table 4. Detonation parameters (calculated using the EXPLO5 code) and initial safety testing data for salts of the $[(\text{CH}_3)_3\text{N}-\text{NH}_2]^+$ cation.

	T_{ex} [K] ^[a]	P_{det} [kbar] ^[b]	D [m s ⁻¹] ^[c]	V_0 [L kg ⁻¹] ^[d]	I_{sp} [s] ^[e]	Impact [J] ^[f]	Friction [N] ^[f]	ESD (+/–) ^[g]	Thermal Shock ^[h]
2	2799	218	7905	883	213	> 50	> 360	–	burns
3 ^[i]	3612	246	7912	818	238	< 40	> 360	–	burns fast
4	1866	132	6790	854	184	> 50	> 360	–	burns
5	1850	181	7468	810	181	> 50	> 360	–	burns
7	3027	190	7208	686	190	> 50	> 360	–	burns slowly
8	3139	228	7947	870	219	< 12	< 30	–	deflagrates
9	2686	201	7595	798	202	< 2	< 48	–	deflagrates
10	3550	260	8176	820	235	< 10	< 20	–	deflagrates

[a] Temperatures of the explosion gases; [b] calculated detonation pressures; [c] calculated detonation velocities; [d] volumes of the explosion gases; [e] specific impulses (calculated for an isobaric combustion at a chamber pressure of 60.0 bar); [f] impact and friction sensitivities (according to BAM methods); [g] rough sensitivities to electrostatic discharge (+ and – indicate sensitive and insensitive, respectively); [h] responses to fast heating in the flame of a Bunsen burner (“flame test”); [i] the detonation parameters (excepting I_{sp}) of compound **3** were calculated for a mixture containing 99% of **3**+1% trifluorotrinitroazhexane (TFNA).

perchlorate salt **3** exhibiting the highest decomposition point at 322 °C. The formation energies of the salts of the $[(\text{CH}_3)_3\text{N}-\text{NH}_2]^+$ cation vary between –698 (**7**) and 1706 (**5**) kJ kg⁻¹ and are approximately between that of the commonly used diaminotrinitrobenzene (DATB), $\Delta_f U^\circ = -403$ kJ kg⁻¹,^[31] and that of the recently reported 1-propargyl-1,1-dimethylhydrazinium dicyanamide ($\Delta_f U^\circ = 1734$ kJ kg⁻¹).^[9] Regardless of being a highly exothermic compound ($\Delta_f U^\circ = 1615$ kJ kg⁻¹), the low crystal density of the azide salt **4** ($\rho = 1.217$ g cm⁻³) accounts for its low detonation pressure and detonation velocity ($P_{det} = 132$ kbar and $D = 6790$ m s⁻¹). On the other hand, the higher density of the nitroformiate salt **10** ($\rho = 1.603$ g cm⁻³) explains the higher detonation parameters of the latter material ($P_{det} = 260$ kbar and $D = 8176$ m s⁻¹). For the remainder of the com-

pounds the detonation pressures are in the range 181 to 246 kbar and the detonation velocities vary between 7208 and 7947 ms⁻¹. By comparison, 2,4,6-trinitrotoluene (TNT) has a detonation pressure of 195 kbar and a detonation velocity of 6881 ms⁻¹.^[31] The specific impulses of the salts of the [(CH₃)₃N-NH₂]⁺ cation in this work are in the range between 181 (**5**) and 238 seconds (**3**) and are comparable to those of recently reported hydrazine-based salts.^[9] Formulations of the compounds in this work with AN and ADN at neutral oxygen ratios have improved the predicted performances in comparison to the stand-alone materials (Supporting Information, Tables S5 and S6). Mixtures with AN have detonation pressures in the range 262 (**4**+AN) to 278 kbar (**3**+AN and **10**+AN), detonation velocities between 8147 (**4**+AN) and 8322 ms⁻¹ (**10**+AN), and specific impulses, which vary between 227 (**4**+AN and **5**+AN) and 236 seconds (**3**+AN). The ADN formulations have higher predicted performances than the AN mixtures ($P_{\text{det}}=334\text{--}343$ kbar, $D=8777\text{--}8953$ ms⁻¹, and $I_{\text{sp}}=248\text{--}255$ s).

We used standard BAM tests (BAM=Bundesanstalt für Materialforschung und -prüfung; Federal Institute for Materials Research and Testing) to assess the sensitivities of all compounds in this work to impact, friction, and electrostatic discharge.^[32–35] All tested materials are insensitive to an electrostatic discharge of approximately 20 kV. Compounds **2–7** are insensitive to impact and friction, whereas the better oxygen-balanced compounds **8–10** are either very sensitive or sensitive to impact and very sensitive towards friction according to the UN recommendations on the transport of dangerous goods^[35] By comparison, TNT has an impact sensitivity of 15 J and a friction sensitivity of 355 N.^[31]

Heats of Explosion and Decomposition Gases

We used the ICT software^[36] to predict the heats of explosion and the decomposition gases of the energetic salts of the [(CH₃)₃N-NH₂]⁺ cation described in this report (Table 5).

In general, for the compounds with an oxygen-based anion, gaseous water is the major predicted decomposition product, followed by the formation of molecular nitrogen. In particular, the nitrogen-rich azide and 5-amino-1*H*-tetrazole salts (compounds **4** and **5**) are predicted to form the

largest amount of nitrogen gas (ca. 350 g kg⁻¹). After water and nitrogen, the main decomposition product is expected to be carbon soot. The amounts are expected to be lower, the less negative the oxygen balance of the materials, so that the better oxygen-balanced perchlorate and dinitramide salts (compounds **3** and **8**) are expected to form less carbon soot (ca. 185 g kg⁻¹). The amounts of ammonia gas predicted are higher for the salts with the non-oxidizing azide and 5-amino-1*H*-tetrazole salts (compounds **4** and **5**, ca. 300 g kg⁻¹) than for the remainder of the compounds containing an oxygen-based anion. The amounts of gases such as CO₂, CO, H₂, CH₄, or HCN are generally low. Formulations of the salts of the [(CH₃)₃N-NH₂]⁺ cation with AN and ADN at approximately neutral oxygen ratios are predicted to form three main decomposition products (Supporting Information, Tables S7 and S8). For the formulations with AN, gaseous water is expected to be the major product (between 437 and 494 g kg⁻¹), followed by nitrogen gas (between 304 and 381 g kg⁻¹) and carbon dioxide (between 124 and 231 g kg⁻¹). On the other hand, the ADN mixtures are expected to decompose forming mainly nitrogen gas (between 366 and 476 g kg⁻¹), followed by water vapor (between 310 and 378 g kg⁻¹) and carbon dioxide (between 158 and 283 g kg⁻¹). The predicted heats of explosion of the pure compounds vary between very low for the nitrogen-rich salts **4** and **5** (ca. 660 cal g⁻¹) to high for the better oxygen-balanced materials **3** and **10** (ca. 1615 cal g⁻¹). Formulations of the compounds with higher heats of explosion with AN are expected to reduce their values in comparison to the stand-alone materials, while salts **4** and **5**, which have lower heats of explosion, are expected to increase their values when formulated with AN. The formulations with ADN generally show a significant increase in the heats of explosion, although the materials with higher heats of explosion (e.g., **3**: 1631 cal g⁻¹) are expected to have slightly lower values when formulated with ADN (**3**+AND: 1605 cal g⁻¹). Commonly used energetic compounds such as 1,3,5-trinitroperhydro-1,3,5-triazine (RDX) have values of about 1590 cal g⁻¹.^[37]

Conclusions

1,1,1-Trimethylhydrazinium iodide ([[(CH₃)₃N-NH₂]⁺I⁻, **1**) was used as a starting material for the synthesis of energetic salts of the [(CH₃)₃N-NH₂]⁺ cation with nitrogen-rich (azide, 5-amino-1*H*-tetrazolate, and 5-nitrotetrazolate) and oxidizing (nitrate, perchlorate, picrate, dinitramide, and nitroformiate) anions. The compounds were fully characterized including X-ray crystal structure determination. The hydrogen-bonding

Table 5. Predicted heats of explosion and decompositions gases of energetic salts of the [(CH₃)₃N-NH₂]⁺ cation.^[a]

Compound	CO ₂	H ₂ O	N ₂	CO	H ₂	NH ₃	CH ₄	HCN	C	ΔH_{ex} [cal g ⁻¹] ^[b]
2	5	387	189	5	5	142	31	1	235	1415
3 ^[c]	16	394	119	8	2	49	10	0.6	191	1631
4	–	–	353	–	8	297	135	1.3	206	670
5	–	–	351	–	6	321	78	1.3	243	649
7	88	328	215	24	2	18	6	0.4	317	1265
8	16	379	320	7	2	80	9	0.8	184	1424
9	3	186	395	3	3	148	30	1	228	1097
10	93	392	292	17	1	22	2	0.5	179	1599

[a] The amount of gases formed at 298 K is given in grams of gas per kilogram of energetic compound; [b] heat of explosion; [c] additionally, HCl (209 g kg⁻¹) was predicted for the perchlorate salt **3**.

networks found in the solid state in the structures of salts **1**, **6**, and **7** were described in the formalism of graph-set analysis. Additionally, we also determined the crystal structure of Ba(NH₄)(NT)₃ (NT=5-nitrotetrazole anion). With the exception of the oxygen-rich dinitramide and nitroformate salts **8** and **10**, the remainder of the materials have good to excellent thermal stabilities up to 322 °C. While compounds **8–10** have relatively high sensitivities towards impact and friction (BAM tests), the rest of the materials are insensitive to the same stimuli. Except for the low-density azide salt **4**, the calculated detonation velocities of all compounds in this work are higher than that of the commonly used TNT, and most of the salts in this work are less sensitive towards classical stimuli than TNT. Lastly, the amounts of toxic gases predicted upon decomposition of salts **2–5** and **7–10** (using the ICT code) are relatively low and are reduced in the case of oxygen-balanced formulations with ammonium nitrate and ammonium dinitramide, which in turn have higher (computed) performances.

Experimental Section

Cautionary Note

Hydrazines and its derivatives are powerful fuels and might react vigorously with certain oxidizers. Many of the compounds handled and described in this work are sensitive and/or potentially explosive materials. Special care needs to be taken, in particular, when working with silver azide and handling compounds **8–10**. Thus, we recommend the handling of these materials to be carried out only by expert personnel and using safety equipment (e.g., Kevlar/leather gloves, Kevlar/leather coat, face shield, and ear plugs).

General Method for the Preparation of Salts **2–6**

The corresponding silver salt, i.e., silver nitrate (0.680 g, 4.0 mmol), silver perchlorate (0.830 g, 4.0 mmol), silver 5-amino-1*H*-tetrazolate (0.921 g, 4.8 mmol), and silver sulfate (0.623 g, 2.0 mmol) was dissolved/suspended in distilled water (10 mL), and neat compound **1** (0.808 g, 4.0 mmol) was added portionwise. The reaction mixture was stirred at room temperature under the exclusion of light for 4 h (compounds **2**, **3**, and **6**) or overnight (compound **5**). The insoluble silver iodide was then removed by filtration and the solvent was removed under reduced pressure and at 40 °C. The crude product was treated as described below.

1,1,1-Trimethylhydrazinium nitrate (**2**)

The crude product was washed twice with THF (2 × 5.0 mL) and twice with diethyl ether (2 × 5.0 mL) and dried under high vacuum to give a colorless crystalline solid (0.527 g, 96%). DSC (5 °C min⁻¹, °C): 258.0 (dec); ¹H NMR ([D₆]DMSO, 400.18 MHz, TMS): δ = 3.26 (9H, s, -CH₃), 6.11 ppm (2H, s(br), -NH₂); ¹³C NMR ([D₆]DMSO, 100.52 MHz, TMS): δ = 57.2 ppm (-CH₃); Raman (rel. int.): ν̄ = 435(4) 461(7) 484(4) 749(89) 910(6) 947(8) 1043(62) 1052(100) 1205(45) 1215(47) 1470(5) 1515(51) 2952(22) 3035 cm⁻¹ (24); IR (golden gate, rel. int.): ν̄ = 3385(w) 3278(m) 3164(m) 3035(w) 1617(m) 1517(vs) 1483(m) 1467(w) 1442(m) 1346(m) 1216(w) 1205(w) 1160(m) 1134(m) 1109(m) 1091(s) 1001(w) 989(w) 947(m) 908(w) 833(w) 785(w) 751(w) 725(w) 710(w) 641(w) 544(w) 506(w) 497(w) 476(w) 468 cm⁻¹ (w); MS *m/z* (ESI⁺): 212.0 (38, [Cat₂A]⁺), 349.1 (63, [Cat₃A₂]⁺), 486.2 (100, [Cat₄A₃]⁺), 623.3 (80, [Cat₅A₄]⁺), 760.3 (58, [Cat₆A₅]⁺), 897.3 (36, [Cat₇A₆]⁺), 1034.5 (52, [Cat₈A₇]⁺), 1171.5 (45 [Cat₉A₈]⁺), 1308.5 (46, [Cat₁₀A₉]⁺), 1445.5 (41, [Cat₁₁A₁₀]⁺), 1582.6 (31 [Cat₁₂A₁₁]⁺), 1720.0 (17, [Cat₁₃A₁₂]⁺), 1857.6 (19, [Cat₁₄A₁₃]⁺); *m/z* (ESI⁻): 198.9 (2, [Cat₂A]⁻), 336.1 (1, [Cat₂A₃]⁻), 473.3 (7, [Cat₃A₄]⁻), 610.5 (13, [Cat₄A₅]⁻), 747.5 (22, [Cat₅A₆]⁻), 884.4 (61, [Cat₆A₇]⁻), 1021.6 (45, [Cat₇A₈]⁻), 1158.4 (64, [Cat₈A₉]⁻), 1295.4 (100, [Cat₉A₁₀]⁻), 1432.7

(27, [Cat₁₀A₁₁]⁻), 1569.6 (29, [Cat₁₁A₁₂]⁻), 1706.7 (33, [Cat₁₂A₁₃]⁻), 1843.7 (31, [Cat₁₃A₁₄]⁻), 1980.7 (28, [Cat₁₄A₁₅]⁻); elemental analysis (%) calcd for C₃H₁₁N₃O₃ (MW = 137.14 g mol⁻¹): C 26.27, H 8.08, N 30.64; found C 26.56, H 8.27, N 30.87.

1,1,1-Trimethylhydrazinium perchlorate (**3**)

The crude product was dissolved in methanol, the insolubles were filtered, and the solvent was removed under reduced pressure to yield a colorless powder (0.659 g, 94%). DSC (5 °C min⁻¹, °C): 322.1 (dec); ¹H NMR ([D₆]DMSO, 400.18 MHz, TMS): δ = 3.24 (9H, s, -CH₃), 6.04 ppm (2H, s(br), -NH₂); ¹³C NMR ([D₆]DMSO, 100.52 MHz, TMS): δ = 57.3 ppm (-CH₃); ¹⁵N NMR ([D₆]DMSO, 50.77 MHz, NH₃) δ/ppm: +128.8 (t, ¹J_{N-H} = 67.7 Hz, -NH₂), +79.7 (s, -N(CH₃)₃); Raman (rel. int.): ν̄ = 423(2) 462(7) 479(4) 627(6) 747(19) 912(6) 935(100) 1097(1) 1461(4) 2976(5) 3045 cm⁻¹ (3); IR (golden gate, rel. int.): ν̄ = 3343(w) 3284(w) 3204(w) 3054(w) 2924(w) 1617(m) 1540(w) 1510(w) 1481(m) 1407(w) 1325(w) 1297(w) 1264(w) 1047(s) 945(s) 901(m) 820(w) 772(w) 746(w) 698(w) 678(w) 650(w) 620(s) 554(w) 544(w) 520(w) 506(w) 468(w) 460 cm⁻¹ (w). MS *m/z* (ESI⁺): 249.0 (53, [Cat₂A]⁺), 423.1 (5, [Cat₃A₂]⁺), 597.2 (66, [Cat₄A₃]⁺), 773.2 (100, [Cat₅A₄]⁺), 945.3 (23, [Cat₆A₅]⁺), 1119.4 (21, [Cat₇A₆]⁺), 1297.1 (48, [Cat₈A₇]⁺), 1471.0 (37 [Cat₉A₈]⁺), 1644.9 (46, [Cat₁₀A₉]⁺), 1818.9 (20, [Cat₁₁A₁₀]⁺); *m/z* (ESI⁻): 273.2 (10, [Cat₂A]⁻), 447.2 (1, [Cat₂A₃]⁻), 623.2 (28, [Cat₃A₄]⁻), 797.1 (40, [Cat₄A₅]⁻), 971.5 (42, [Cat₅A₆]⁻), 1145.6 (56, [Cat₆A₇]⁻), 1321.4 (33, [Cat₇A₈]⁻), 1495.3 (41, [Cat₈A₉]⁻), 1671.3 (100, [Cat₉A₁₀]⁻), 1845.4 (43, [Cat₁₀A₁₁]⁻); elemental analysis (%) calcd for C₃H₁₁N₃ClO₄ (MW = 174.58 g mol⁻¹): C 20.64, H 6.35, N 16.05; found C 20.47, H 6.18, N 15.79.

1,1,1-Trimethylhydrazinium 5-amino-1*H*-tetrazolate (**5**)

The crude product was treated in the same way as the nitrate salt **2** (0.567 g, 89%). DSC (5 °C min⁻¹, °C): 250.1 (dec); ¹H NMR ([D₆]DMSO, 400.18 MHz, TMS): δ = 3.28 (9H, s, -CH₃), 3.99 (2H, s(br), C-NH₂), 6.39 ppm (2H, s(br), N-NH₂); ¹³C NMR ([D₆]DMSO, 100.52 MHz, TMS): δ = 57.1 (-CH₃), 164.2 ppm (C-NH₂); Raman (rel. int.): ν̄ = 407(1) 486(1) 499(2) 708(2) 749(17) 900(1) 911(3) 1046(100) 1461(4) 2958(6) 3040 cm⁻¹ (4); IR (golden gate, rel. int.): ν̄ = 3288(w) 3145(w) 3049(w) 3014(w) 1608(m) 1483(m) 1433(w) 1318(m) 1288(m) 1203(w) 1154(w) 1109(w) 1050(s) 942(vs) 895(s) 829(m) 811(w) 772(w) 745(m) 688(w) 670(w) 630(w) 591(w) 573(w) 526(w) 497(w) 476(w) 469 cm⁻¹ (w). MS *m/z* (ESI⁺): 234.0 (100, [Cat₂A]⁺), 393.2 (11, [Cat₃A₂]⁺), 552.5 (6, [Cat₄A₃]⁺), 711.7 (4, [Cat₅A₄]⁺); *m/z* (ESI⁻): 242.9 (6, [Cat₂A]⁻), 402.5 (3, [Cat₂A₃]⁻), 561.6 (46, [Cat₃A₄]⁻), 720.8 (80, [Cat₄A₅]⁻), 879.7 (91, [Cat₅A₆]⁻), 1038.7 (100, [Cat₆A₇]⁻), 1198.0 (59, [Cat₇A₈]⁻), 1357.0 (56, [Cat₈A₉]⁻); Raman (rel. int.): ν̄ = 407(1) 486(1) 499(2) 708(2) 749(17) 900(1) 911(3) 1046(100) 1461(4) 2958(6) 3040 cm⁻¹ (4); IR (golden gate, rel. int.): ν̄ = 3288(w) 3145(w) 3049(w) 3014(w) 1608(m) 1483(m) 1433(w) 1318(m) 1288(m) 1203(w) 1154(w) 1109(w) 1050(s) 942(vs) 895(s) 829(m) 811(w) 772(w) 745(m) 688(w) 670(w) 630(w) 591(w) 573(w) 526(w) 497(w) 476(w) 469 cm⁻¹ (w); elemental analysis (%) calcd for C₄H₁₃N₇ (MW = 159.19 g mol⁻¹): C 30.18, H 8.23, N 61.59; found C 30.02, H 8.11, N 61.17.

General Method for the Preparation of the Barium Salt

The barium salts of dinitramide, 5-nitrotetrazole, and nitroform were prepared by the reaction of ammonium dinitramide, ammonium 5-nitrotetrazolate, and hydrazinium nitroformate, respectively, with half an equivalent of barium hydroxide octahydrate and used “in situ” for the reactions below.

General Method for the Preparation of Salts **7–10**

The corresponding barium salt, i.e., barium picrate tetrahydrate (1.331 g, 2.0 mmol), barium dinitramide (0.699 g, 2.0 mmol), barium 5-nitrotetrazolate (0.731 g, 2.0 mmol), and barium nitroformate (0.875 g, 2.0 mmol) was dissolved/suspended in distilled water (10 mL) and neat compound **6**·2H₂O (0.565 g, 2.0 mmol) was added portionwise. The reaction mixture was stirred at room temperature for 2 h and the insoluble barium sulfate was filtered through a plug of Celite. The solvent was then removed

under reduced pressure and at 40 °C, yielding the crude product, which was treated as described below.

1,1,1-Trimethylhydrazinium picrate (7)

The crude product was recrystallized from hot water yielding single crystals of the compound suitable for the X-ray experiments (1.067 g, 88%). DSC (5 °C min⁻¹, °C): 238.0 (mp), 263.6 (dec); ¹H NMR ([D₆]DMSO, 400.18 MHz, TMS): δ = 3.25 (9H, s, -CH₃), 6.09 (2H, s(br), N-NH₂), 8.59 ppm (2H, s, Ar-H); ¹³C NMR ([D₆]DMSO, 100.52 MHz, TMS): δ = 160.7 (C1), 141.8 (C2), 125.2 (C3), 124.1 (C4), 57.2 ppm (-CH₃); Raman (rel. int.): ν̄ = 214(3) 330(11) 520(4) 707(9) 745(3) 821(90) 924(4) 942(31) 1074(2) 1165(7) 1257(24) 1309(75) 1329(73) 1347(100) 1365(57) 1430(2) 1496(4) 1556(11) 2975(1) 3048 cm⁻¹ (1); IR (golden gate, rel. int.): ν̄ = 3326(w) 3156(w) 3078(w) 1631(m) 1609(s) 1567(s) 1547(s) 1516(s) 1481(s) 1426(m) 1362(s) 1325(vs) 1264(vs) 1163(s) 1109(m) 1072(s) 942(m) 911(s) 835(w) 820(w) 787(m) 743(s) 702(vs) 593(w) 554(w) 514(w) 497(w) 490(w) 468 cm⁻¹ (w). MS *m/z* (ESI⁺): 377.9 (3, [Cat₂A]⁺), 1286.8 (5, [Cat₃A₄]⁺); *m/z* (ESI⁻): 228.1 (100, [A]⁻), 479.0 (6, [2A⁻+Na⁺]⁻), 530.9 (19, [Cat₂A]⁻), 708.0 (21, [3A⁻+Na⁺+H⁺]⁻), 729.7 (7, [3A⁻+2Na⁺]⁻); elemental analysis (%) calcd for C₉H₁₃N₅O₇ (MW = 303.23 g mol⁻¹): C 35.65, H 4.32, N 23.09; found C 35.48, H 4.21, N 22.86.

1,1,1-Trimethylhydrazinium dinitramide (8)

The crude product was treated twice with isopropanol (2.5 mL) and subsequently evaporated to dryness (0.629 g, 87%). DSC (5 °C min⁻¹, °C): 155.4 (dec); ¹H NMR ([D₆]DMSO, 400.18 MHz, TMS): δ = 3.25 (9H, s, -CH₃), 6.07 ppm (2H, s(br), N-NH₂); ¹³C NMR ([D₆]DMSO, 100.52 MHz, TMS): δ = 57.3 ppm (-CH₃); Raman (rel. int.): ν̄ = 298(11) 381(3) 483(12) 747(87) 827(100) 952(17) 1046(15) 1328(92) 1450(8) 1527(3) 2977(11) 3045 cm⁻¹ (6); IR (golden gate, rel. int.): ν̄ = 3316(w) 3196(w) 3048(w) 1624(w) 1518(m) 1481(m) 1425(m) 1333(w) 1170(s) 1087(w) 1009(s) 945(m) 910(w) 826(w) 758(m) 726(w) 688(w) 679(w) 602(w) 573(w) 553(w) 497(w) 484(w) 469 cm⁻¹ (w). MS *m/z* (ESI⁺): 256.0 (98, [Cat₂A]⁺), 437.1 (47, [Cat₃A₂]⁺), 618.2 (100, [Cat₄A₃]⁺), 799.2 (56, [Cat₅A₄]⁺), 980.0 (51, [Cat₆A₅]⁺), 1161.2 (64, [Cat₇A₆]⁺), 1342.2 (84, [Cat₈A₇]⁺), 1523.2 (36, [Cat₉A₈]⁺); *m/z* (ESI⁻): 287.1 (13, [Cat₂A]⁻), 468.0 (3, [Cat₂A₃]⁻), 649.5 (46, [Cat₃A₄]⁻), 830.7 (32, [Cat₄A₅]⁻), 1011.6 (53, [Cat₅A₆]⁻), 1192.7 (90, [Cat₆A₇]⁻), 1373.7 (87, [Cat₇A₈]⁻), 1554.4 (100, [Cat₈A₉]⁻), 1735.5 (77, [Cat₉A₁₀]⁻), 1916.4 (46, [Cat₁₀A₁₁]⁻); elemental analysis (%) calcd for C₃H₁₁N₅O₅ (MW = 181.15 g mol⁻¹): C 19.89, H 6.12, N 38.66; found C 19.73, H 5.87, N 38.42.

1,1,1-Trimethylhydrazinium 5-nitrotetrazolate (9)

The pale yellow liquid obtained after concentration in vacuum was treated as described above for compound 8 to yield a colorless powder (0.692 g, 91%). In one reaction illustrating the synthesis of compound 9, ammonium 5-nitrotetrazolate was reacted with an equivalent amount of barium hydroxide octahydrate to form barium 5-nitrotetrazolate, which was reacted in situ with an equivalent amount of compound 6-H₂O. The crude product was then dissolved in methanol and stored in an ether chamber yielding single crystals of Ba(NH₄)(NT)₃, which were used for the X-ray experiments. DSC (5 °C min⁻¹, °C): 175.3 (dec); ¹H NMR ([D₆]DMSO, 400.18 MHz, TMS): δ = 3.26 (9H, s, -CH₃), 6.10 ppm (2H, s(br), N-NH₂); ¹³C NMR ([D₆]DMSO, 100.52 MHz, TMS): δ = 168.7 (C-NO₂), 57.3 ppm (-CH₃); Raman (rel. int.): ν̄ = 548(3) 753(3) 845(9) 1024(51) 1060(47) 1167(3) 1320(6) 1423(100) 1535(4) 2981(2) 3043 cm⁻¹ (1); IR (golden gate, rel. int.): ν̄ = 3235(m) 3145(m) 3038(w) 2851(w) 1645(w) 1542(s) 1485(m) 1467(m) 1439(s) 1413(s) 1315(s) 1295(w) 1167(m) 1149(w) 1106(m) 1057(w) 1023(w) 949(m) 922(w) 834(vs) 749(w) 667(m) 553(vw) 512(w) 491(w) 471(w) 461 cm⁻¹ (w); MS *m/z* (ESI⁺): 263.9 (100, [Cat₂A]⁺), 453.1 (42, [Cat₃A₂]⁺), 642.1 (62, [Cat₄A₃]⁺), 831.2 (68, [Cat₅A₄]⁺), 1020.2 (64, [Cat₆A₅]⁺), 1209.3 (63, [Cat₇A₆]⁺), 1398.3 (98, [Cat₈A₇]⁺), 1587.3 (33, [Cat₉A₈]⁺), 1776.3 (19, [Cat₁₀A₉]⁺); *m/z* (ESI⁻): 303.1 (14, [Cat₂A]⁻), 492.5 (7, [Cat₂A₃]⁻), 681.5 (71, [Cat₃A₄]⁻), 870.6 (66, [Cat₄A₅]⁻), 1059.7 (38, [Cat₅A₆]⁻), 1248.6 (100, [Cat₆A₇]⁻), 1437.7 (58, [Cat₇A₈]⁻), 1626.6 (61, [Cat₈A₉]⁻), 1815.5 (46, [Cat₉A₁₀]⁻); elemental analysis (%) calcd for C₄H₁₁N₇O₂ (MW = 189.17 g mol⁻¹): C 25.40, H 5.86, N 51.83; found C 25.18, H 6.01, N 51.57.

1,1,1-Trimethylhydrazinium nitroformate (10)

The crude product was treated in the same way as the dinitramide salt 8 (0.801 g, 89%). DSC (5 °C min⁻¹, °C): 106.9 (dec); ¹H NMR ([D₆]DMSO, 400.18 MHz, TMS): δ = 3.25 (9H, s, -CH₃), 6.09 ppm (2H, s(br), -NH₂); ¹³C NMR ([D₆]DMSO, 100.52 MHz, TMS): δ = 57.2 (-CH₃), 150.7 ppm (C-NO₂); Raman (rel. int.): ν̄ = 251(3) 463(2) 495(3) 748(5) 788(7) 868-(100) 1148(11) 1271(14) 1378(15) 1464(3) 2973(2) 3047 cm⁻¹ (1); IR (golden gate, rel. int.): ν̄ = 3318(w) 3198(w) 1623(w) 1534(m) 1477(s) 1402(m) 1372(m) 1249(s) 1142(s) 1072(m) 946(w) 909(w) 866(w) 786(s) 731(s) 565(w) 544(w) 521(w) 497(w) 484(w) 468 cm⁻¹ (w); MS *m/z* (ESI⁺): 299.9 (56, [Cat₂A]⁺), 525.1 (31, [Cat₃A₂]⁺), 750.1 (26, [Cat₄A₃]⁺); *m/z* (ESI⁻): 150.1 (16, [A]⁻), 375.0 (4, [Cat₂A]⁻), 600.1 (2, [Cat₂A₃]⁻), 825.3 (7, [Cat₃A₄]⁻), 1050.5 (4, [Cat₄A₅]⁻), 1275.0 (3, [Cat₅A₆]⁻), 1500.2 (5, [Cat₆A₇]⁻); elemental analysis (%) calcd for C₄H₁₁N₅O₆ (MW = 225.16 g mol⁻¹): C 21.34, H 4.92, N 31.10; found 21.11, H 4.70, N 30.79.

Acknowledgements

Financial support by the CNRS (Centre Nationale de la Recherche Scientifique) and the University Claude Bernard of Lyon are gratefully acknowledged.

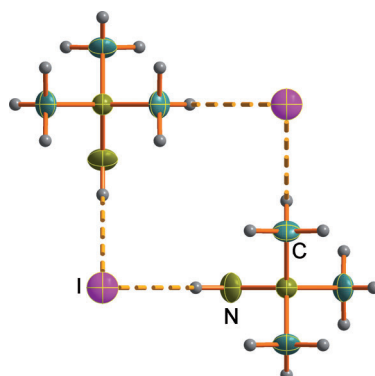
- [1] C. Nonnenberg, I. Frank, T. M. Klapötke, *Angew. Chem.* **2004**, *116*, 4686–4689; *Angew. Chem. Int. Ed.* **2004**, *43*, 4586–4589.
- [2] L. Catoire, N. Chaumeix, C. Paillard, *J. Propul. Power* **2004**, *20*, 87–92.
- [3] L. Catoire, N. Chaumeix, S. Pichon, C. Paillard, *J. Propul. Power* **2006**, *22*, 120–126.
- [4] A. Osmont, L. Catoire, T. M. Klapötke, G. L. Vaghjiani, M. T. Swihart, *Propellants Explos. Pyrotech.* **2008**, *33*, 209–212.
- [5] International Conference on Green Propellant for Space Propulsion, 20–22 June **2001**, Noordwijk, The Netherlands: <http://esamultimedia.esa.int/conferences/01a05/index.html>.
- [6] a) Y. Zhang, J. M. Shreeve, *Angew. Chem.* **2011**, *123*, 965–967; *Angew. Chem. Int. Ed.* **2011**, *50*, 935–937; b) L. He, G.-H. Tao, D. A. Parrish, J. M. Shreeve, *Inorg. Chem.* **2011**, *50*, 679–685; c) Y. Huang, Y. Zhang, J. M. Shreeve, *Chem. Eur. J.* **2011**, *17*, 1538–1546.
- [7] a) T. M. Klapötke, C. Miró Sabaté, *Chem. Mater.* **2008**, *20*, 1750–1763; b) T. M. Klapötke, C. Miró Sabaté, A. Penger, M. Rusan, J. M. Welch, *Eur. J. Inorg. Chem.* **2009**, 880–896; c) T. M. Klapötke, C. Miró Sabaté, *Z. Anorg. Allg. Chem.* **2009**, *635*, 1812–1822; d) M.-J. Crawford, T. M. Klapötke, F. A. Martin, C. Miró Sabaté, M. Rusan, *Chem. Eur. J.* **2011**, *17*, 1683–1695.
- [8] a) H. Gao, Y.-H. Joo, B. Twamley, Z. Zhou, J. M. Shreeve, *Angew. Chem.* **2009**, *121*, 2830–2833; *Angew. Chem. Int. Ed.* **2009**, *48*, 2792–2795; b) V. Forquet, C. Darwich, C. Miró Sabaté, H. Delalu, *Proceed. 13th Sem. New Trends in Res. Energ. Mater.* (Pardubice, Czech Republic) **2010**.
- [9] Y. Zhang, H. Gao, Y. Guo, Y.-H. Joo, J. M. Shreeve, *Chem. Eur. J.* **2010**, *16*, 3114–3120.
- [10] P. F. Pagoria, G. S. Lee, A. R. Mitchell, R. D. Schmidt, *Thermochim. Acta* **2002**, *384*, 187–204.
- [11] H. Xue, J. M. Shreeve, *Adv. Mater.* **2005**, *17*, 2142–2146.
- [12] M. Freemantle, *Chem. Eng. News* **2007**, *85*, 23–26.
- [13] G. Steinhäuser, T. M. Klapötke, *Angew. Chem.* **2008**, *120*, 3376–3394; *Angew. Chem. Int. Ed.* **2008**, *47*, 3330–3347.
- [14] C. Miró Sabaté, H. Delalu, *Eur. J. Inorg. Chem.* **2012**, 866–877.
- [15] C. Miró Sabaté, E. Jeanneau, H. Delalu, *Chem. Asian J.* **2012**, *7*, 1085–1095.
- [16] H. H. Sisler, G. Omietanski, *Inorg. Synth.* **1957**, *5*, 91–95.
- [17] G. A. Olah, M. B. Sassaman, M. Zuanic, C. B. Rao, G. K. S. Prakash, *J. Org. Chem.* **1992**, *57*, 1585–1588.
- [18] a) T. Haberer, A. Hammerl, G. Holl, T. M. Klapötke, J. Knizek, H. Nöth, *Eur. J. Inorg. Chem.* **1999**, 849–852; b) A. Hammerl, G.

- Holl, M. Kaiser, T. M. Klapötke, P. Mayer, H. Piotrowski, M. Vogt, *Z. Naturforsch. B* **2001**, *56*, 847–856.
- [19] a) K. Williamson, P. Li, J. P. Devlin, *J. Chem. Phys.* **1968**, *48*, 3891–3896; b) J. R. Fernandes, S. Ganguly, C. N. R. Rao, *Spectrochim. Acta Part A* **1979**, *35*, 1013–1019.
- [20] a) H. Cohn, *J. Chem. Soc.* **1952**, 4282–4284; b) P. Redlich, J. Holt, T. Biegeleisen, *J. Am. Chem. Soc.* **1944**, *66*, 13–16; c) H. Grothe, H. Willner, *Angew. Chem.* **1996**, *108*, 816–818; *Angew. Chem. Int. Ed. Engl.* **1996**, *35*, 768–769.
- [21] K. Karaghiosoff, T. M. Klapötke, P. Mayer, C. Miró Sabaté, A. Penger, J. M. Welch, *Inorg. Chem.* **2008**, *47*, 1007–1019.
- [22] C. Miró Sabaté, E. Jeanneau, J. Stierstorfer, *Z. Anorg. Allg. Chem.* **2011**, *637*, 1490–1501.
- [23] T. M. Klapötke, P. Mayer, J. Stierstorfer, *Phosphorus Sulfur Silicon Relat. Elem.* **2009**, *184*, 2393–2407.
- [24] T. M. Klapötke, C. Miró Sabaté, *Z. Anorg. Allg. Chem.* **2008**, *634*, 1017–1024.
- [25] T. M. Klapötke, C. Miró Sabaté, J. M. Welch, *Dalton Trans.* **2008**, 6372–6380.
- [26] M. Göbel, T. M. Klapötke, *Z. Anorg. Allg. Chem.* **2007**, *633*, 1006–1017.
- [27] N. B. Colthup, L. H. Daly, S. E. Wiberley, *Introduction to Infrared and Raman Spectroscopy*, Academic Press, Boston, **1990**.
- [28] J. A. Pople, R. Seeger, R. Krishnan, *Int. J. Quantum Chem. Symp.* **1977**, *11*, 149.
- [29] a) J. Bernstein, R. E. Davis, L. Shimoni, N. Chang, *Angew. Chem.* **1995**, *107*, 1689–1708; *Angew. Chem. Int. Ed. Engl.* **1995**, *34*, 1555–1573; b) <http://www.ccdc.cam.ac.uk/support/documentation/rpluto/TOC.html>.
- [30] a) M. Sućeska, *Propellants Explos. Pyrotech.* **1991**, *16*, 197; b) M. Sućeska, *Propellants Explos. Pyrotech.* **1999**, *24*, 280.
- [31] J. Köhler, R. Meyer, *Explosivstoffe*, 9th ed., Wiley-VCH, Weinheim, Germany, **1998**.
- [32] <http://www.bam.de>; <http://www.reichel-partner.de>.
- [33] a) NATO standardization agreement (STANAG) on explosives, impact sensitivity tests, no. 4489, Ed. 1, Sept. 17, **1999**; b) NATO standardization agreement (STANAG) on explosive, friction sensitivity tests, no. 4487, Ed. 1, Aug. 22, **2002**.
- [34] *WIWEB-Standardarbeitsanweisung 4-5.1.03, Ermittlung der Explosionsgefährlichkeit oder der Reibeempfindlichkeit mit dem Reibeapparat*, Nov. 8, **2002**.
- [35] Impact: Insensitive > 40 J, less sensitive ≥ 35 J, sensitive ≥ 4 J, very sensitive ≤ 3 J; friction: Insensitive > 360 N, less sensitive = 360 N, sensitive 80–360 N, very sensitive ≤ 80 N, extremely sensitive ≤ 10 N. According to the UN Recommendations on the Transport of Dangerous Goods (+) indicates: not safe for transport.
- [36] a) *ICT-Thermodynamic Code, Version 1.0*, Fraunhofer-Institut für Chemische Technologie (ICT): Pfinztal, Germany, 1988–2000; b) R. Webb, M. van Rooijen, *Proceed. 29th Int. Pyrotech. Sem.*, Westminster, CO, **2002**, pp. 823–828; c) H. Bathelt, F. Volk, *27th Int. Ann. Conf. ICT*, **1996**, *92*, 1–16.
- [37] T. M. Klapötke, C. Miró Sabaté, M. Rasp, *J. Mater. Chem.* **2009**, *19*, 2240–2252.

Received: May 16, 2012
Published online: ■ ■ ■, 0000

FULL PAPER

Bursting with energy: 1,1,1-Trimethylhydrazinium iodide (see figure) was used as a starting material for the synthesis of energetic salts with nitrogen-rich and oxidizing anions. Many of the compounds have excellent thermal stabilities, low sensitivities towards classical stimuli, and performance values higher than the commonly used 1,3,5-trinitrotoluene (TNT).



Energetic Salts

Carles Miró Sabaté,* Henri Delalu,
Erwann Jeanneau ————— ■■■■-■■■■

Energetic Hydrazine-Based Salts with Nitrogen-Rich and Oxidizing Anions 